7 ON STACKING

Martin Egli

Department of Biochemistry, Vanderbilt University, Nashville, Tennessee 37232, USA
Fax 1-615-322-7122, E-mail martin.egli@vanderbilt.edu

Abstract   The term 'stacking' is normally associated with π-π interactions between aromatic moieties. The parallel alignment between adjacent DNA bases arguably constitutes the best-known example and provides the dominating contribution to the overall stability of DNA duplexes. Beyond canonical π-π interactions, a preliminary inspection of crystal structures of nucleic acids and their complexes with proteins reveals a wealth of additional stacking motifs including edge-to-face, H-π, cation-π, lone pair-π and anion-π interactions. Given the ubiquity and diversity of such motifs it seems reasonable to widen the meaning of stacking beyond the standard cofacial interactions between pairs of aromatics.

7.1 Introduction

Stacking interactions between aromatics are commonly dubbed π-π contacts, but considered separately from the underlying framework of σ-bonds, the dominant interaction resulting from closely approaching π clouds would be a repulsive one. Some twenty years ago Hunter and Sanders developed several simple rules to characterize the nature of π-π interactions,[1] i.e. (i) π-π repulsion dominates a face-to-face π-stacked geometry; (ii) π-σ attraction dominates an edge-on or T-shaped geometry; (iii) π-σ attraction dominates in an offset π-stacked geometry; (iv) in contacts involving polarized π systems, charge-charge interactions dominate. We note that the authors are differentiating between two parallel relative orientations of stacked bases: Face-to-face leading to maximum overlap and cofacial but slipped. This simple electrostatic model accounted for many of the experimental observations with stacking, for example that maximum π-overlap that would be favored by solvophobic effects is rarely observed. Thus, the electrostatic contribution is dominant as far as the geometry of the stacking interaction is concerned. Van der Waals interactions make an appreciable contribution but cannot override electrostatics, as cofacial arrangements between aromatics with no offset would otherwise be prevalent. Therefore, although other contributions to the total energy of the interaction besides electrostatics, such as induction (polarization), dispersion and repulsion can play an important role, in the absence of significant

stabilizing effects by polarization, cofacial-offset or edge-on geometries will be preferred over face-to-face alignments. Crystal structures of nucleic acids are highly instructive regarding the former [2-4] in that base overlap is modulated by helical twist, and the observed stacking interactions between bases in DNA [5] (Fig. 7.1A) and presumably also in RNA duplexes (Fig. 7.1B) support the above electrostatic model.

Although there is no agreement as to the dominant influence on the stacking strength and the importance of the electrostatic contribution,[6-11] clever PAGE assays with asymmetrically nicked and base-gapped DNAs were recently used to partition the contributions by base stacking and pairing (Watson-Crick hydrogen bonds) to the overall stability of duplex DNA.[12] These data leave no doubt that base stacking is the main stabilizing factor in the DNA duplex, triggering a major paradigm shift in the interplay of forces that hold the duplex together. This is because the higher thermodynamic stability of pairing between DNA strands with increasing GC-content is normally attributed to the influence of three hydrogen bonds in G:C compared to the two in A:T pairs. However, the research by Frank-Kamenetskii and coworkers demonstrated that base stacking is always stabilizing for both GC- and AT-containing contacts in the duplex. Conversely, base pairing between G and C does not contribute to stability and the pairing between A and T is actually destabilizing in the overall context. Further, the effects of salt concentration and temperature on stacking resemble the dependences of the total thermodynamic stability of DNA duplexes on the two parameters. In other words, it is the dependence of the stacking component of stability on both these parameters that determines their influence on the overall stability. This is remarkable as is the insight, that for all temperatures, heterogeneities in stacking related to GC- versus AT-involving interactions make up at least half of the heterogeneity of the total stability. The other half is the result of the different energetics of G:C and A:T pairing. The contribution of stacking to the stability of a polynucleotide in the single-stranded state has recently been measured for oligo(dA) by atomic-force spectroscopy and amounts to ca. 3.6 kcal/mol per adenine base ([13] and cited references). More extensive stacking is most likely also the reason behind the significantly higher stability of an artificial nucleic acid pairing system (xDNA) with size-expanded base pairs compared with native DNA.[14] Clearly there are countless other examples that support the importance of stacking for stability that are not cited or discussed here in detail.

With stacking thus emerging as the chief contributor to the stability of the DNA double helix, it is reasonable to review different types of stacking beyond the standard interactions between bases in nucleic acid duplexes, interactions involving aromatic moieties in crystal structures of proteins including edge-on contacts between oxygen atoms and Phe [15] and those between hydrogen bond donors and the face of π-systems,[16-18] or the cofacial, edge-on and coplanar pairing types of aromatics in the crystals of small organic molecules.[19,20] The examples presented in this brief review are taken mostly from crystal structures of native DNA and RNA and chemically modified nucleic acid systems and are certainly not meant to provide an exhaustive account of this topic. Moreover, the description is

mostly qualitative and experimental data for the stability of the individual interactions or estimates based on semi-empirical computations are cited wherever available but are not explicitly provided here.

7.2 Intra- and inter-strand base stacking

Adjacent base pairs in DNA and RNA duplexes provide excellent examples for the cofacial-offset stacking type. Helical twist that amounts to 36° and 33° in the canonical B-form DNA and A-form RNA duplex forms along with shifts (see ref. [21] for a definition of helical parameters) that preclude face-to-face orientations of bases. But DNA and RNA exhibit very different types of stacking that are related to the conformational preferences of the sugar moiety in their backbones. The ribose in double-stranded RNA adopts the C3′-*endo* pucker and the 2′-deoxyribose in B-form DNA adopts the C2′-*endo* pucker.[2] This leads to the base pairs being inclined relative to the helical axis in RNA whereas DNA base pairs are orientated in a more or less perpendicular fashion relative to the helical axis. Thus, in the illustrations of DNA and RNA base-pair steps in Fig. 7.1, the helical axis for DNA coincides approximately with the vertical direction. However, the axis in RNA is inclined relative to the base pair planes. An important consequence of the chemical and conformational differences between DNA and RNA is the relative slip of stacked base pairs along their long dimension. As can be seen in Fig. 7.1A, DNA stacking is mostly of the intra-strand type. By comparison, the RNA duplex is virtually devoid of overlap between bases from the same strand and instead the stabilization is due to inter-strand stacking. This is particularly obvious at 5′-pyrimidine-purine-3′ steps, for example the 5′-CpG-3′ step depicted in Fig. 7.1B.

The pairing stability of RNA strands significantly exceeds that of the corresponding DNA strands and is the result of a favorable enthalpy term.[24] However, RNA duplexes exhibit a more extensive hydration compared with DNA and this difference is directly associated with the presence of 2′-hydroxyl groups in the RNA minor groove.[25] This renders the entropy term of the free energy of pairing unfavorable in the case of RNA. Unfortunately, it is not straightforward to partition the individual contributions, i.e. base stacking, base pairing and hydration, to the overall pairing stability of RNA. Assays to determine the relative importance of stacking and pairing like those reported for DNA [12] have not been carried out with RNA to my knowledge. So although we are aware of the different stacking patterns in DNA and RNA duplexes, it is initially unclear how significant this difference is with regard to the higher pairing stability of the latter. Comparison between the experimentally determined stability increases due to dangling ends (an unpaired base either at the 5′- or the 3′-end) in DNA and RNA duplexes ([26] and cited refs.) supports the notion that inter-strand stacking provides higher stability. Similar experimental data for the (2′-4′)-linked pyranosyl-RNA (pRNA)

analog that exhibits even more pronounced inter-strand stacking than RNA are also in line with this conclusion.[27]
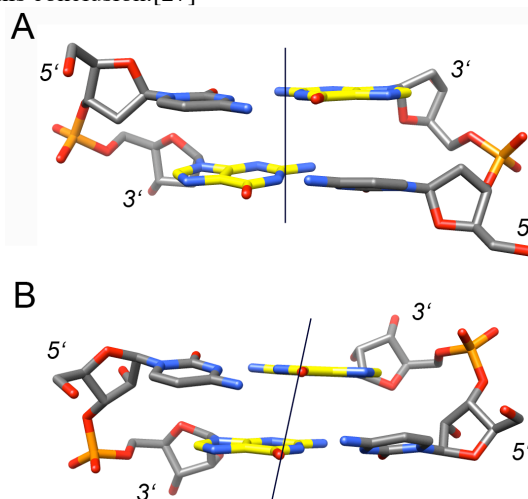
Fig. 7.1. Base stacking in DNA and RNA. (A) CpG base pair step in a B-form DNA duplex (Dickerson-Drew dodecamer, PDB ID code 436D [22]). (B) CpG base pair step in an A-form RNA duplex (dodecamer with G:A mismatches, PDB ID code 2Q1R [23]). The views are into the major groove and carbon atoms of guanine bases are highlighted in yellow to illustrate the different degrees of inter-strand stacking in the two duplex types. Thin solid lines indicate the approximate orientations of the helical axes.

7.3 Parallel and perpendicular intercalating agents

Planar aromatic compounds can insert themselves between DNA or RNA base pairs and thereby pry them apart. The intercalator takes on the role of a base pair and its π-face overlaps extensively with the base pairs above and below, the latter now separated by about 6.8 Å or twice the typical distance between stacked base pairs. Intercalation does not lead to disruption of Watson-Crick hydrogen bonds. Simple chromophores intercalate such that their long axis runs more or less parallel to the long axis of the surrounding base pairs. The dyes ethidium bromide [28] and acridine orange [29] are well-known examples of so-called parallel intercalators [30] (Fig. 7.2A). Parallel intercalation is usually accompanied by unwinding of the duplex and the sugar pucker and backbone torsion angles need to adapt in order to bridge the wider step.[2] Intercalator and flanking base pairs are typically aligned so as to maximize overlap; electrostatics and van der Waals interactions likely dominate the energetics of the parallel intercalation mode.
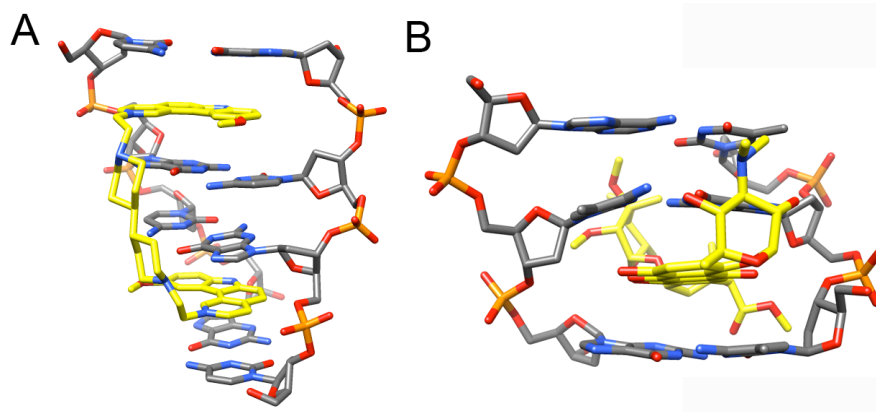
Fig. 7.2. Parallel and perpendicular intercalators. (A) The bis-intercalating drug ditercalinium in complex with the duplex [d(CGCG)]$_2$ exemplifies the parallel stacking type (PDB ID code 1D32 [31]). (B) Nogalamycin intercalates at the CpG base pair steps in the duplex [d(CGTACG)]$_2$ and is representative of the perpendicular intercalation mode (PDB ID code 1D17 [32]). Both duplexes are viewed into the major groove and carbon atoms of drug molecules are highlighted in yellow.

By comparison, more extensive conformational distortions in DNA are observed upon intercalation of chromophores that feature bulky substituents. The presence of a sugar moiety, as in the anthracycline antibiotics daunorubicin and doxorubicin (anticancer agents), prevents a parallel intercalation mode.[33] Thus, the chromophore is forced to rotate and enter the base-pair stack in a perpendicular mode. This places the substituent in the groove where it can engage in hydrogen bonds to donors and acceptors on the base edges. Nogalamycin differs from the more common daunorubicin-type anthracyclines in that it is substituted on both ends of the intercalating chromophore and thus takes on the shape of a dumbbell (Fig. 7.2B).[32] The bicyclic amino sugar that carries a positively charged dimethylamino group is fused to one side and is located in the major groove upon intercalation where it forms hydrogen bonds to N7 of G and N4 of C. The nogalose sugar at the other end enters the minor groove but no hydrogen bonds are established. However, the carbonyl oxygen of the methylester substituent that also resides in the minor groove is hydrogen bonded to the exocyclic amino group of the terminal G (Fig. 7.2B). Unlike parallel intercalators that unwind the DNA at the site of intercalation, the unwinding caused by these so-called perpendicular intercalators occurs at the adjacent base-pair step.[30] Other consequences of parallel intercalation include concerted changes in the α and γ backbone torsion angles.[34] Moreover, the perpendicular intercalation mode is often accompanied by severe buckling of base pairs that wrap around the chromophore. This leads to partial unstacking on one side but may allow for more optimal relative orientations of acceptors and donors on nucleobases and intercalator for hydrogen bond formation. In place of the cofacial-offset stacking type seen with parallel intercalators, exocyclic keto and hydroxyl groups of the nogalamycin

aglycone are tilted relative to the π-faces of bases on one side (Fig. 7.2B). Therefore, the parallel and perpendicular intercalator modes differ distinctly and perpendicular intercalators display a mixture of hydrogen bonding and cofacial and edge-on stacking to bind to DNA.

7.3.1 Cofacial versus edge-on stacking

Simple aromatics such as benzene can pair via cofacial and edge-on stacking and the stabilities afforded by these interaction modes are likely very similar.[20] Unlike the π-systems in benzene or in phenylalanine those in the nucleobases are polarized as a result of their heterocyclic nature and the presence of exocyclic substituents. In addition backbone constraints and regular parallel π-stacking in DNA duplexes render edge-on interactions of bases very unlikely. Moreover, in crystals of oligonucleotides or protein-DNA complexes end-to-end stacking by duplexes of the cofacial-offset type constitutes the most common packing motif. The single-stranded nature of RNA permits considerably more structural variety but stems (double helical portions) make up much of the secondary structure and the parallel stacking type is prevalent.
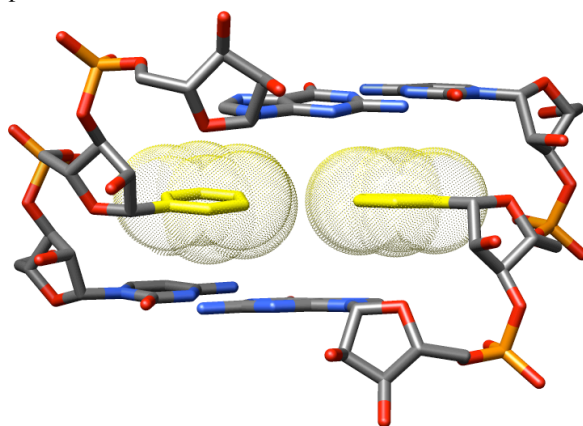
Fig. 7.3. 'Pairing' of phenyl-ribonucleotides (p) in the center of the RNA duplex [r(CCCpGGGG)]₂ (PDB ID code 1G2J [35]). The dotted surfaces illustrate that phenyl rings from opposite strands are virtually in van der Waals contact.

We were interested in the consequences of incorporation of simple aromatic moieties as far as the geometry of stacking interactions is concerned. In one study we analyzed the conformational properties of an RNA octamer CCCpGGGG with an incorporated phenyl-ribonucleotide (p). In the crystal structure, strands pair such that a configuration with a phenyl ring placed opposite a G is avoided.[35] Instead phenyls 'pair' under formation of a 3′-dangling G (Fig. 7.3). This arrangement generates a seamless π-stack and repulsive contacts to nucleobases are

avoided by isolating the hydrophobic phenyl moieties in the core of the duplex. Despite potentially favorable hydrophobic and van der Waals interactions resulting from the phenyl pair, incorporation of a single p residue in an RNA leads to drastically reduced stability of pairing. In the case of the octamer duplex, the melting temperature was reduced by 35°C ($\Delta G°_{37} \approx +7.5$ kcal/mol) relative to the native [r(CCCCGGGG)]$_2$ duplex.[35]

In comparison to the phenyl-modified RNA duplex, the crystal structure of a DNA duplex with stilbenediether (Sd, Fig. 7.4A) caps revealed multiple stacking types (Fig. 7.4).[36] One of the two hairpin molecules per crystallographic asymmetric unit displayed a parallel offset orientation (Fig. 7.4B). In the second molecule, the stilbene's planarity was lost; the dihedral angle between phenyl rings amounted to 10°. One of the phenyls was partially unstacked from the neighboring G and the other adopted an edge-on orientation relative to C (Fig. 7.4C). Unlike the phenyl moieties in the RNA duplex discussed above, the Sd linkers are located at the end of a duplex and are free to interact with one another in the crystal lattice. For example, in the structure of an Sd-capped DNA duplex co-crystallized with Sr^{2+}, four Sd moieties engaged in a pinwheel-like arrangement, featuring exclusively edge-on type stacking.[37] This observation reinforces the view that simple aromatics can easily switch between the parallel and edge-on stacking modes. Unlike the aforementioned phenyl-ribonucleotide the Sd linker greatly stabilizes DNA duplexes.
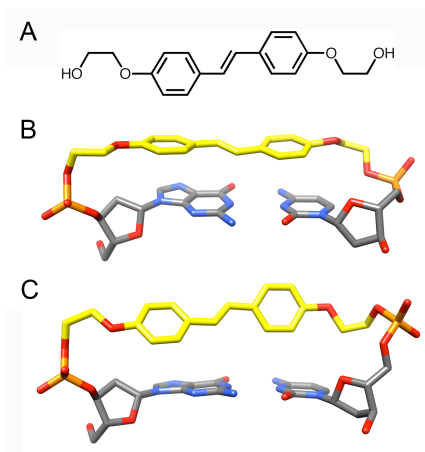
Fig. 7.4. Conformations of a stilbene diether moiety (Sd) that caps the DNA hairpin d(GTTTG)-se-d(CAAAAC) (PDB ID code 1PUY [36]). (A) Structure of Sd. (B) Canonical stacking of Sd on the adjacent C:G base pair. The trans-stilbene portion of Sd adopts a planar conformation (C) Unstacked (phenyl ring on the left) and edge-on interaction with the cytosine below (phenyl ring on the right) of Sd in the second DNA hairpin per crystallographic asymmetric unit.

7.4 Base-backbone inclination and sugar-base stacking

(4′→6′)-Linked oligo-2′,3'-dideoxy-β-*D*-glucopyranose nucleic acid (homo-DNA) was studied as part of research directed at an etiology of nucleic acid structure.[38,39] Homo-DNA was considered an autonomous pairing system until recently, i.e. homo-DNA oligonucleotides do not pair with DNA and RNA or any of the artificial nucleic acid analogs. The only exception identified to date is L-cyclohexanyl nucleic acid (L-CNA) that forms a left-handed duplex with homo-DNA [40].
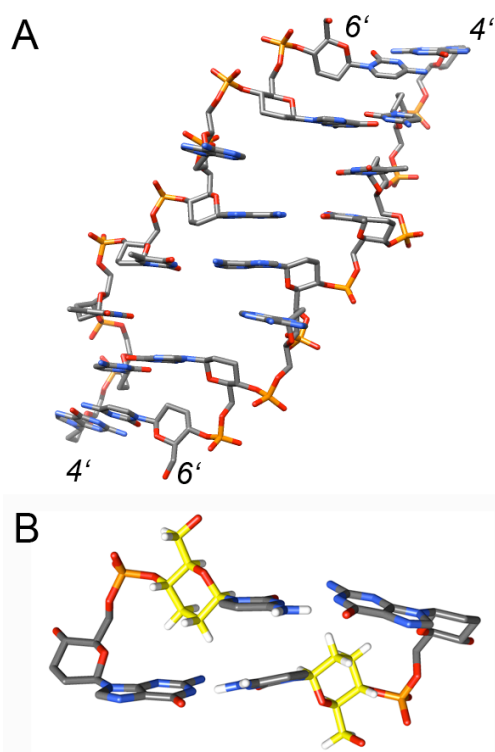
Fig. 7.5 Structure of homo- (hexose-) DNA. (A) The crystal structure of the homo-DNA duplex 6′-[dd(CGAATTCG)]₂-4′ viewed into the major groove (PDB ID code 2H9S [41]). Nucleotides A3 in the first strand and A11 in the second are looped out and interact with a neighboring duplex, whereby adenosines from the latter insert themselves into the gaps created. In the crystal lattice homo-DNA duplexes form tightly interacting dimers. (B) H-π type sugar-base stacking: Hydrogen atoms of 2′,3′-dideoxyglucopyranoses (highlighted in yellow) point into the adjacent nucleobase. The illustration depicts the (C1:G16)p(G2:C15) base pair step.

The crystal structure of a homo-DNA octamer duplex showed a right-handed helix with average values for rise and twist of 3.8 Å and 14°, respectively, and a highly irregular geometry (Fig. 7.5A).[41] Strongly inclined backbone and base-pair axes are one of the hallmarks of the homo-DNA duplex. Unlike RNA in

which backbones and base-pair planes exhibit a negative inclination (ca. –30°), the inclination angle in homo-DNA is positive (ca. 45° on average [41-43], Fig. 7.5). Thus, stacking between adjacent base pairs is exclusively of the inter-strand type in homo-DNA. As Fig. 7.5 illustrates there is virtually no overlap between adjacent bases from the same strand.

Owing to a favorable entropic contribution, the pairing stability of homo-DNA oligonucleotides exceeds that of DNA by far.[44] This property is consistent with the reduced conformational flexibility of the hexose sugar compared with $2'$-deoxyribose. The exceptionally large slide between adjacent base pairs combined with the limited helical twist result in another unique feature of the homo-DNA duplex: sugar-nucleobase stacking (Fig. 7.5B). Instead of the standard intra-strand π-π stacking seen in B-DNA, the $2',3'$-dideoxyglucopyranose of the $6'$-nucleotide sits directly above the nucleobase of the $4'$-nucleotide and equatorial $C2'$-H bonds of the former are pointing into the π-face. Although the sugar-base stack may involve mainly van der Waals interactions (distances between $C2'$ atoms from the sugar and the best plane through base atoms are as short as 3.1 Å), it is unlikely to be repulsive. In any case, the extensive inter-strand base stacking characteristic of homo-DNA, will likely offset any destabilizing consequences of the close approach between sugar and nucleobase. A recent report by Leumann and colleagues appears to provide evidence that C-H$\cdots\pi$ stacking contacts between a saturated hydrocarbon and a phenyl moiety are not merely tolerated but may actually be stabilizing.[45] Thus they analyzed the thermodynamic stability of DNA duplexes with 1-3 phenylcyclohexyl-C-nucleoside pairs incorporated into their center and found the modification to be associated with an increase in duplex stability. The higher stability is enthalpic in nature and seems to arise from cyclohexyl$\cdots$phenyl interactions.

7.4.1 Amino acid-nucleobase stacking

Interactions between OH or NH donors and the π-faces of aromatic side chains in amino acids were analyzed extensively in the crystal structures of proteins [16,18]. Such interactions are ubiquitous and it is intuitively clear that a short contact between a donor functionality and a negatively polarized π-system can be stabilizing. Another motif seen quite frequently involves C-H moieties and the π-faces of aromatic acid side chains or nucleobases [46]. Two examples are depicted in Fig. 7.6. At the active site of death-associated protein kinase (DAPk), the C_δ methyl group of a methionine points directly into the six-membered ring of adenine from ATP (Fig. 7.6A,B) [47]. All kinases (DAPk belongs to the family of Ser/Thr kinases) bind ATP, but they catalyze the transfer of the ATP γ-phosphate to different targets. Although the ATP-binding pockets of different kinases exhibit certain similarities, they deviate from each other to various degrees to allow for the

observed specificity of the kinase reaction. Thus, an apparently minor contact like the one depicted in Fig. 7.6A,B may well make a subtle contribution to specificity.
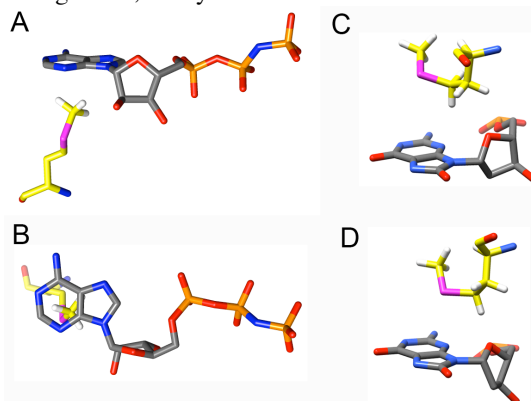
Fig. 7.6. H-π type amino acid-nucleobase stacking motifs. Met···ATP (AMPPnP) in the crystal structure of death associated protein kinase (DAPk, PDB ID code 1IG1 [47]). (A) Viewed from the side, and (B) rotated by ca. 90° around the horizontal axis and viewed approximately along the normal to the aromatic moiety. Met···8oxoG in the crystal structure of the human Pol-kappa (hPolκ) DNA complex (PDB ID code 2W7P [48]). (C) The amino acid-base stack in one of the two complexes per crystallographic asymmetric unit, and (D) the interaction in the second complex. Carbon atoms of methionine are highlighted in yellow and the sulfur atom is highlighted in magenta.

At the active site of the human trans-lesion DNA polymerase-kappa (hPol κ) in complex with a DNA template-primer construct containing an 8-oxoG adduct, we observed another type of Met···nucleobase stacking (Fig. 7.6C,D). The methionine side chain snakes along the base plane of 8-oxoG, whereby the relative orientations of amino acid and nucleobase differ only minimally in the two complexes per crystallographic asymmetric unit. This arrangement leads to various C-H···π contacts between Met methylene groups and the 8-oxoG base moiety. In addition, the sulfur atom exhibits a distance of ca. 3.1 Å from the best plane through nucleobase atoms in both complexes, well below the sum of van der Waals radii for carbon (1.7 Å) and sulfur (1.8 Å). The Met···8-oxoG stacking interaction likely stabilizes the *syn* conformation of the adducted nucleotide, thus leading to incorrect insertion of dATP opposite 8-oxoG.

7.5 Stacked dipoles: The C-rich i-motif

Cytidine-rich (C-rich) DNAs form a four-stranded arrangement, whereby two parallel-stranded duplexes intercalate (i-motif) into each other such that their backbones run into opposite directions [49,50] (Fig. 7.7A,B). The tetraplex is held together by interdigitated, hemiprotonated C:C$^+$ base pairs that are rotated by about 90° between neighboring planes (Fig. 7.7C). One of the striking features of the i-

motif is the absence of overlap between the six-membered rings of Cs from neighboring base pairs. Instead the main contribution to stability likely comes from stacks of dipoles with an antiparallel orientation (δ+ C_2=O2 δ- / δ- O_2=C2 δ+). If we further consider a tautomeric form of C^+ with the positive charge on the exocyclic N4 amino group, additional stability would be provided by this charge being positioned above the π cloud of the cytosine underneath (Fig. 7.7C). Thus, there must be a significant electrostatic contribution to the stability of the C-rich i-motif, consistent with the presence of hemiprotonated C:C^+ base pairs. Additional contributions to the stability of the i-motif may stem from a network of C-H···O4′ hydrogen bonds between adjacent 2′-deoxyriboses from antiparallel strands (Fig. 7.7).[51] It is noteworthy that T-rich oligonucleotides cannot form a self-intercalated four-stranded structure analogous to that adopted by C-rich strands. The pK_a of N3 of C (5′-nucleotide) is ca. 4.6 and the nucleobase is therefore protonated under slightly acidic conditions (summarized in [52]). Thymine on the other hand is neutral as the pK_a of N3 is ca. 10.5 (5′-nucleotide).
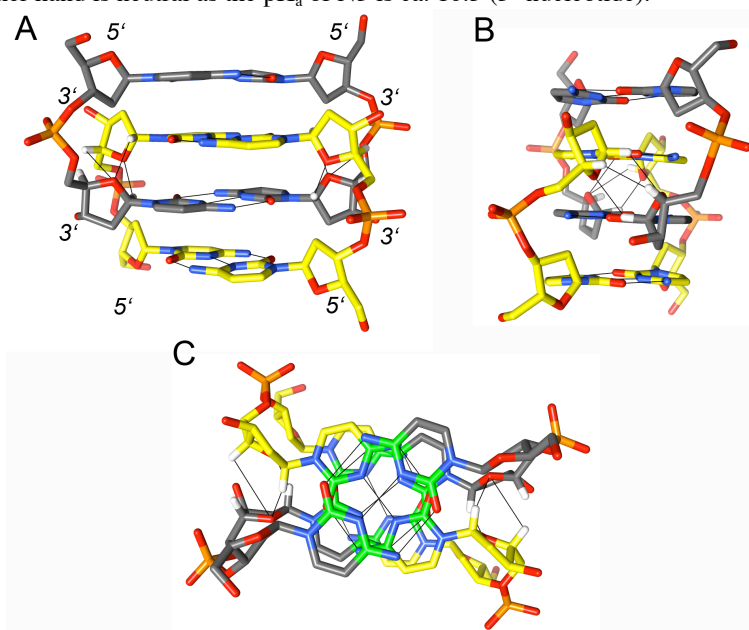
Fig. 7.7. Crystal structure of the central portion of the four-stranded self-intercalated i-motif formed by the DNA tetramer d(CCCC) (PDB ID code 190D [50]). Carbon atoms in the parallel-stranded duplex whose strands run from top to bottom are colored in gray and those in the duplex with strands running in the opposite direction are colored in yellow. (A) The tetraplex viewed into a major groove. (B) Rotated by ca. 90° around the vertical axis and viewed into a minor groove. (C) Rotated by ca. 90° around the horizontal axis (relative to panel A) and viewed down the stack of hemi-protonated C:C^+ base pairs, illustrating the lack of an overlap between cytosine six-membered rings. Pairs of C4-N4(H_2) and C2=O2 moieties that are aligned in an antiparallel fashion (C2 and C4 carbon atoms are highlighted in green) may instead contribute significantly to the overall stability of the i-motif. Hydrogen bonds in cytosine pairs and C-H···O4′ interactions between 2′-deoxyribose sugars across the minor groove are shown as thin solid lines.

7.6 Cation-π interactions

It should come as no surprise that cations can interact favorably with the π-face of an aromatic system.[53,54] In their analysis of the nature of π-π interactions, Hunter and Sanders discussed the optimum geometry of the porphyrin-porphyrin pair.[1] Accordingly, the most stable configuration is one where the pyrrole ring of one porphyrin is located under the π-cavity at the center of the other. Metalla-tion places a positive charge in the central cavity and results in a favorable inter-action with the π-electrons of the adjacent pyrrole ring, thus enhancing porphyrin aggregation. Another nice example of a cation-π stacking interaction is found in the structure of a DNA-protein complex (Fig. 7.8).[55] The Ndt80 protein uses ar-ginines to interact with the major groove edge of Gs from the same strand in the 5′-TGTG sequence motif. This sequence-specific Arg···G interaction is present in virtually every protein-DNA complex. The guanidinium moiety of Arg is proto-nated at neutral pH and in addition to probing the major groove edge of G, the protein uses the positive charge to pull thymines out of the base-pair stack (Fig. 7.8). Thus, the guanidinium moiety engages in a cofacial contact with T and in addition the Arg Cβ methylene group forms a hydrophobic contact with the 5-methyl group of the nucleobase. The Ndt80 complex attests to the never-ending repertoire that proteins rely on to establish sequence-specific interactions with DNA, in this case by using Arg to not only gauge the separation between two Gs in the major groove, but to also exploit the particular conformational plasticity of the TpG step(s).
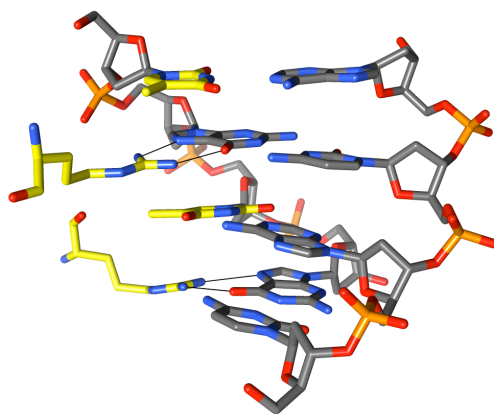
Fig. 7.8. Cation-π interactions in the crystal structure of the yeast sporulation regulator Ndt80 in complex with DNA (PDB ID code 1MNN [55]). A pair of arginines interacts with the major groove edges of guanines whereby the guanidinium moiety from Arg stacks onto the 5′-adjacent T. The protein uses the formation of these Arg-T stacks to specifically recognize the tandem 5′-TpG-3′ sequence motif. The view is into the major groove, hydrogen bonds are shown as thin solid lines, and carbon atoms of arginine and thymine are highlighted in yellow.

7.7 Lone pair-π and anion-π interactions

Unlike cation-π interactions those between lone electron pairs (lp) or anions and the π-faces of aromatic systems may initially seem counterintuitive. Of course, an H-π interaction, say, involving water and benzene or tryptophan is energetically favorable compared to a configuration with the water oxygen located above the center of the aromatic ring and directing its lone pair(s) into the π-cloud. However, when the aromatic system is strongly polarized, as in hexafluorobenzene,[56] or carrying a positive charge, i.e. protonated imidazole,[57] the lp-π interaction can result in a significant stabilization. In terms of electrostatics, the H-π interaction involves the HOMO of the aromatic ring and the LUMO of water ($\pi \rightarrow \sigma^*$) and the lp-π interaction involves the HOMO of water and the LUMO of the aromatic ring ($n \rightarrow \pi^*$).[58-60]

Many years ago, we described the conserved $2'$-deoxyribose (cytidine)···guanine stack in crystal structures of the left-handed Z-DNA duplex [d(CGCGCG)]$_2$ [58]. Unlike with homo-DNA where the hexose is positioned above the adjacent nucleobase such that a C-H moiety points into the π-system, it is the α lone pair of the sugar O4$'$ atom that is directed into the six-membered ring of guanine (Fig. 7.9A). In left-handed Z-DNA the helical twist alternates between high and low values for neighboring base-pair steps and C and G exhibits different conformations of the sugar. At CpG steps there is a virtual absence of overlap between the cytosine and guanine base planes and the sugar of the former takes the place of the nucleobase instead (Fig. 7.9A). The distance between the 4$'$-oxygen and the best plane defined by guanine atoms varies between 2.82 and 2.96 Å in the structures of the so-called magnesium, spermine and mixed magnesium/spermine crystal forms [61] of the left-handed hexamer. At the time we interpreted the close approach of the sugar as an $n(O4') \rightarrow \pi^*(C2=N2H_2^+)$ interaction (see inset in Fig. 7.9A). We based our assumption of a tautomeric form of G with N2 and O6 being positively and negatively charged, respectively, on the frequently observed coordination of Mg^{2+} to the major groove edge of G in Z-DNA crystals. Distances between O4$'$(C) and C2(G) vary between 2.90 and 3.09 Å in the crystal structures and are thus similar to the distances between the oxygen and the G-plane. CG-repeats show a particular propensity for adopting the left-handed duplex type and insertion of TpA steps destabilizes the formation of the Z-duplex.[62] Adenine cannot mimic the particular polarization of guanine in Z-DNA and the stabilizing contribution as a result of the sugar-base stack at CpG steps [63] will be at best neutral at a TpA step. The stacking arrangement between a 2$'$-deoxyribose and guanine is a hallmark of Z-DNA and provided early support for the existence of lp-π interactions in biological systems.
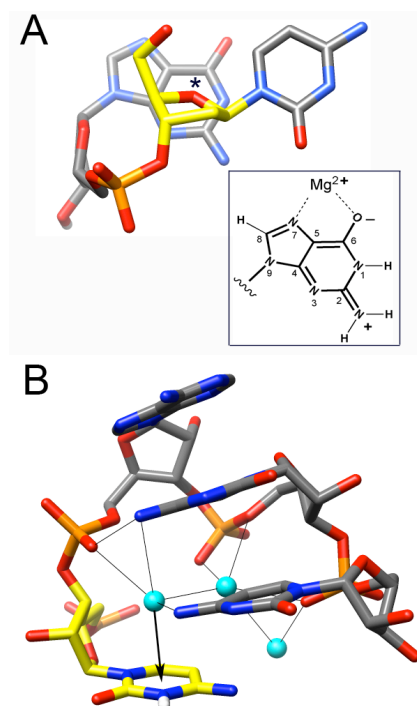
Fig. 7.9. Lone pair-π (lp-π) stacking. (A) The lp-π stacking motif at CpG steps in the crystal structure of the left-handed Z-DNA duplex [d(CGCGCG)]₂ (PDB ID code 131D [64]). The 2′-deoxyribose of cytidine (carbon atoms highlighted in yellow) is lodged above the guanine base, resulting in an interaction between a 4′-oxygen (asterisk) lone pair and the positively polarized ring portion of G (the inset depicts a tautomeric form of G relevant in the case of lp-π stacking). (B) The C-turn in the crystal structure of the −1 frameshifting RNA pseudoknot from beet western yellow virus (BWYV pkRNA, PDB ID code 1L2X [65]). A water molecule (highlighted in cyan) sits directly above a protonated cytidine (yellow). The particular environment of this water molecule (neighboring hydrogen bond donor and acceptor moieties) and the tight spacing between the water oxygen atom and the aromatic plane are consistent with an lp(oxygen)-π(C) interaction (indicated by the arrow).

Another striking example of an lp-π interaction is found in the C-loop of a −1 ribosomal frameshifting pseudoknot RNA (pk-RNA). There, a water molecule sits directly above a protonated cytosine, and our conclusion that one of the oxygen lone pairs points into the π-face of the nucleobase is supported by the tight distance (2.93 Å; Fig. 7.9B) and the particular distribution of hydrogen-bond acceptor and donor moieties around this water molecule.[66] We know that the cytosine is protonated from the particular pairing geometry of the base observed in the crystal structure of the pk-RNA at atomic resolution.[65] Calculations performed at various levels of theory provide a consistent picture, namely that lp-π interactions yield substantial stabilization when the aromatic moiety is strongly polarized or, as in the above case, positively charged.[57,63,67] Naturally, it would be very interesting to conduct a neutron diffraction study with crystals of the pk-RNA as

this would allow visualization of the position of hydrogen (deuterium) atoms and also permit a better characterization of other potential lp-π and several H-π interactions in the crystal.[66] In addition to the Z-DNA and pk-RNA examples, we recently reviewed other types of lp-π interactions involving carbonyl oxygens and aromatics.[63] Based on an analysis of protein crystal structures others have recently found numerous occurrences of close interactions between carbonyl oxygens and the side chains of aromatic amino acids with a geometry that is between those of ideal π-π and lp-π stacking interactions.[60] Obviously many more examples of lp-π type stacking interactions will emerge in the structures of small and macro molecules in the coming years as closer attention is being paid to novel types of weak interactions (for example refs. [68,69]).

The aforementioned cases of lp-π interactions involve neutral species (i.e. 2′-deoxyribose O4′, water, or carbonyl oxygen), but there are others in which the moiety contributing the lone pair is negatively charged. For example in the so-called U-turn RNA tertiary structural motif,[70] a phosphate group sits above a uracil base, an interaction that may contribute favorably to stability thanks to the particular polarization of U.[63] However, there are also numerous examples of anion-π interactions in the structures of small molecules (for example refs. [71-75]).

7.8 Unique properties of the TATA-motif major groove

Hydrogen bonding and stacking play crucial roles in determining the stability and three-dimensional structure of the DNA double helix. Although we often treat them as separate entities - Watson-Crick hydrogen bonds linking nucleobases more or less perpendicularly to the helix axis and π-π interactions coupling nucleobases along the direction of the axis - it is clear that the electrostatics of hydrogen bonding affect the stacking geometry and thus the sequence-dependent shape of the double helix and its recognition by proteins. It is normally assumed that base moieties are perfectly planar, but theoretical and experimental studies have provided support for out-of-plane positions of hydrogen atoms from amino groups.[76-80] Bifurcated hydrogen bonding involving adenine and thymine across adjacent levels from the stack have also been reported in DNA crystal structures [81] and analyzed with theoretical means.[82] In addition bifurcated cross-strand hydrogen bonding between non-planar amino groups from A and C and A and A from adjacent base pairs has also invoked.[83-85] However, the resolutions of crystal structures of macromolecules typically do not allow visualization of hydrogen atoms, and the degree of a potential out-of-plane perturbation of the exocyclic adenine, guanine and cytosine amino groups therefore has not been settled based on crystallographic data.
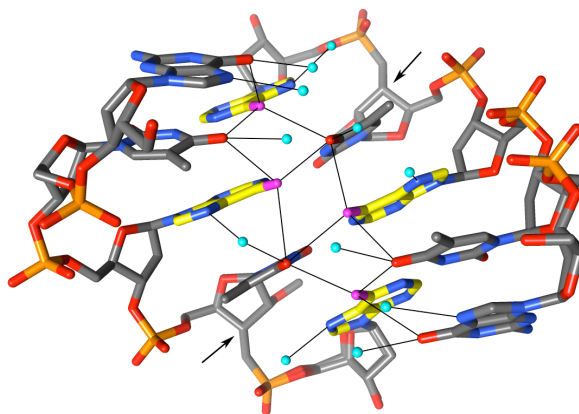
Fig. 7.10. Major groove hydration in the central TATA portion of the DNA duplex [dGCGTA-tACGC]₂ (t=2′-methoxy-3′-methylene-T, see arrows) visualized at atomic resolution (0.83 Å, PDB ID code 1DPL [86]). All potential hydrogen bond (thin solid lines) acceptor moieties of nucleobases near the floor of the groove (O4 of T and N7 of A) engage in contacts to water (cyan spheres), whereas exocyclic N6 amino groups (magenta) from adenines (carbon atoms colored in yellow) are not associated with water. Instead adenines engage in bifurcated hydrogen bonds to paired (Watson-Crick) and stacked thymines, thus apparently limiting the capability of N6(A) to interact with solvent molecules. Superimposed sugar moieties of the adenosine residue visible near the bottom edge of the Fig. indicate a crystallographic disorder.

The major groove of the central TATA tetramer in the crystal structure of an A-form DNA duplex exhibits a remarkable hydration pattern [86]: All acceptor functions from bases with the exception of adenine $N6H_2$ form hydrogen bonds to water molecules (Fig. 7.10). The absence of waters associated with these exocyclic amino groups is initially puzzling, but closer inspection of the major groove indicates that N6(A), in addition to being hydrogen bonded to O4 from the T it pairs with, also appears to establish a hydrogen bond to O4 from the 3′-adjacent T. Fig. 7.10 also depicts hydrogen bonds between N6(A) and O4 from the 5′-adjacent T because the distances between N6(A) and O4(3′-T) and N6(A) and O4(5′-T) are similar. Without knowledge of the positions of hydrogen atoms, it is not straightforward to settle the geometry of the hydrogen-bond network. However, the potential formation of such bifurcated hydrogen bonds is facilitated by the sliding of adjacent base pairs in the A-form environment and the high propeller twist of A:T pairs. In turn, bifurcated hydrogen bonds will affect the geometry of the duplex and the particular shape of the TATA-repeat. This motif is contained in the TATA-box sequence that is usually located 25 base pairs upstream to the transcription site which is recognized by RNA polymerase II as part of a multi-protein complex [87]. Although the energetic consequences of the network of hydrogen bonds in the major groove of the TATA sequence are not understood in detail, the thought that bifurcated hydrogen bonds could influence its geometry and the recognition by the TATA-binding protein (TBP, [88] and refs. cited) is intriguing.

7.9 Conclusion

In this brief overview I have provided examples of various types of stacking, the term stacking designating the relative orientation of a chemical moiety interacting with an aromatic system whereby the former sits above the π-face of the latter either in the face-to-face or cofacial-offset modes. Instead of a somewhat narrow use of 'stacking' as an interaction between π-systems of parallel orientation and forces that are mainly dispersive in nature, stacking here simply refers to moieties, including aromatics, hydrocarbons, cations, anions, water, etc., interacting with the π-cloud of an aromatic system. The resulting catalog of interactions shows a considerable range of stacking-type supramolecular building blocks. The nature of these interactions is decidedly Coulombic in some cases and thus different from parallel stacks between the side chains of aromatic amino acids or nucleobases of various polarizations. Compared to the familiar stacking of base-pairs in DNA, lone pair-π, cation-π, and anion-π stacking and interactions between hydrocarbons such as sugars and the π-faces of aromatic systems have not been analyzed in a systematic way. It is likely that many more examples of such interactions can be retrieved from the three-dimensional structures of proteins and RNAs, as those described here merely represent cases over which we and others had stumbled in a more or less fortuitous manner. A particularly interesting example of a non-standard stacking interaction, of the cation-π type, has recently been demonstrated to be at the origin of the higher affinity for nicotine by acetylcholine receptors in the brain (thought to underlie nicotine addiction) relative to receptors in the muscle.[89] The last item reviewed here, the potential role of non-planar amino groups in the formation of bifurcated hydrogen bonds that affect the stacking geometry and stability of macromolecular assemblies, i.e. DNA duplexes, would undoubtedly profit from single-crystal neutron diffraction studies. The renewed interest in neutron diffraction with crystals of macromolecules in recent years and the availability of spallation sources that permit the use of smaller crystals raise the possibility that we may be able to gather experimental evidence for or against the non-planarity of amino groups in the near future.

REFERENCES

1. Hunter, C. A.; Sanders, J. K.M., *J. Am. Chem. Soc.* **1990**, *112*, 5525–5534.
2. Saenger, W., Principles of nucleic acids structure. Springer Verlag, New York, **1984**.
3. Berman, H. M.; Olson, W. K.; Beveridge, D. L.; Westbrook, J.; Gelbin, A.; Demeny, T.; Hsieh, S.-H.; Srinivasan, A. R.; Schneider, B., *Biophys. J.* **1992**, *63*, 751–759 (http://ndbserver.rutgers.edu).
4. Neidle, S., Principles of nucleic acids structure. Academic Press, London, **2008**.
5. Hunter, C. A.; Lu, X.-J., *J. Mol. Biol.* **1997**, *265*, 603–619.
6. Hunter, C. A., *J. Mol. Biol.* **1993**, *230*, 1025–1054.

194

7.   Newcomb, L. F.; Gellman, S. H., *J. Am. Chem. Soc.* **1994**, *116*, 4493–4494.
8.   Friedman, R. A.; Honig, B., *Biophys. J.* **1995**, *69*, 1528–1535.
9.   Guckian, K. M.; Schweitzer, B. A.; Ren, R.X.-F. Sheils, C.J.; Tahmassebi, D. C.; Kool, E. T., *J. Am. Chem. Soc.* **2000**, *122*, 2213–2222.
10. Luo, R.; Gilson, H. S.; Potter, M. J.; Gilson, M. K., *Biophys. J.* **2001**, *80*, 140–148.
11. Sponer, J.; Leszczynski, J.; Hobza, P., *Biopol.* **2001**, *61*, 3–31.
12. Yakovchuk, P.; Protozanova, E.; Frank-Kamenetskii, M. D., *Nucleic Acids Res.* **2006**, *34*, 564–574.
13. Ke, C.; Humeniuk, M.; Gracz, H. S.; Marszalek, P. E., *Phys. Rev. Lett.* **2007**, *99*, 018302-1–018302-4.
14. Liu, H.; Gao, J.; Kool, E. T., *J. Am. Chem. Soc.* **2005**, *127*, 1396–1402.
15. Thomas, K. A.; Smith, G. M.; Thomas, T. B.; Feldmann, R. J., *Proc. Natl. Acad. Sci. U.S.A.* **1982**, *79*, 4843–4847.
16. Burley, S. K.; Petsko, G. A., *FEBS Lett.* **1986**, *203*, 139–143.
17. Burley, S. K.; Petsko, G. A., *Advan. Protein Chem.* **1988**, *39*, 125–189.
18. Steiner, T.; Koellner, G., *J. Mol. Biol.* **2001**, *305*, 535–557.
19. Desiraju, G. R., *Angew. Chem. Int. Ed. Engl.* **1995**, *34*, 2311–2327.
20. Dunitz, J. D.; Gavezzotti, A., *Angew. Chem. Int. Ed. Engl.* **2005**, *44*, 1766–1787.
21. Dickerson, R. E., *Nucleic Acids Res.* **1998**, *26*, 1906–1926.
22. Tereshko, V.; Minasov, G.; Egli, M., *J. Am. Chem. Soc.* **1999**, *121*, 470–471.
23. Li, F.; Pallan, P. S.; Maier, M. A.; Rajeev, K. G.; Mathieu, S. L.; Kreutz, C.; Fan, Y.; Sanghvi, J.; Micura, R.; Rozners, E.; Manoharan, M.; Egli, M., *Nucleic Acids Res.* **2007**, *35*, 6424–6438.
24. Egli, M., *Angew. Chem. Int. Ed. Engl.* **1996**, *35*, 1894–1909.
25. Egli, M.; Portmann, S.; Usman, N., *Biochem.* **1996**, *35*, 8489–8494.
26. Bommarito, S.; Peyret, N.; SantaLucia Jr., J., *Nucleic Acids Res.* **2000**, *28*, 1929–1934.
27. Micura, R.; Bolli, M.; Windhab, N.; Eschenmoser, A., *Angew. Chem. Int. Ed. Engl.* **1997**, *36*, 870–873.
28. Jain, S. C.; Tsai, C. C.; Sobell, H. M., *J. Mol. Biol.* **1977**, *114*, 317–331.
29. Wang, A. H. J.; Quigley, G. J.; Rich, A., *Nucleic Acids Res.* **1979**, *6*, 3879–3890.
30. Williams, L. D.; Egli, M.; Gao, Q.; Rich, A., In: Structure & function: proceedings of the seventh conversation in biomolecular stereodynamics (Sarma, R. H.; Sarma, M. H., eds.) Adenine Press, Albany, NY, pp 107–125, **1992**.
31. Gao, Q.; Williams, L. D.; Egli, M.; Rabinovich, D.; Chen, S. L.; Quigley, G. J.; Rich, A., *Proc. Natl. Acad. Sci. U.S.A.* **1991**, *88*, 2422–2426.
32. Egli, M.; Williams, L. D.; Frederick, C. A.; Rich, A., *Biochem.* **1991**, *30*, 1364–1372.
33. Frederick, C. A.; Williams, L. D.; Ughetto, G.; van der Marel, G. A.; van Boom, J. H.; Rich, A.; Wang, A. H. J., *Biochem.* **1990**, *29*, 2538–2549.
34. Egli, M**,** In: Structure correlations (Dunitz, J. D.; Bürgi, H. B., eds.) VCH-Publishers, Weinheim, Vol 2, pp 705–749, **1994**.
35. Minasov, M.; Matulic-Adamic, J.; Wilds, C. J.; Haeberli, P.; Usman, N.; Beigelman, L.; Egli, M., *RNA* **2000**, *6*, 1516–1528.
36. Egli, M.; Tereshko, V.; Murshudov, G. N.; Sanishvili, R.; Liu, X.; Lewis, F. D., *J. Am. Chem. Soc.* **2003**, *125*, 10842–10849.
37. Lewis, F. D.; Liu, X.; Wu, Y.; Miller, S.; Wasielewski, M. R.; Letsinger, R. L.; Sanishvili, R.; Joachimiak, A.; Tereshko, V.; Egli, M., *J. Am. Chem. Soc.* **1999**, *121*, 9905–9906.
38. Eschenmoser, A.; Dobler, M., *Helv. Chim. Acta* **1992**, *75*, 218–259.
39. Eschenmoser, A., *Chem. Commun.* **2004**, 1247–1252.
40. Froeyen, M.; Morvan, F.; Vasseur, J. J.; Nielsen, P.; van Aerschot, A.; Rosemeyer, H.; Herdewijn, P., *Chem. Biodivers.* **2007**, *4*, 803–817.
41. Egli, M.; Pallan, P. S.; Pattanayek, R.; Wilds, C. J.; Lubini, P.; Minasov, G.; Dobler, M.; Leumann, C. J.; Eschenmoser, A., *J. Am. Chem. Soc.* **2006**, *128*, 10847–10856.
42. Egli, M.; Lubini, P.; Pallan, P. S., *Chem. Soc. Rev.* **2007**, *36*, 31–45.
43. Pallan, P. S.; Lubini, P.; Bolli, M.; Egli, M., *Nucleic Acids Res.* **2007**, *35*, 6611–6624.

44. Hunziker, J.; Roth, H. J.; Böhringer, M.; Giger, A.; Diedrichsen, U.; Göbel, M.; Krishnan, R.; Jaun, B.; Leumann, C.; Eschenmoser, A., *Helv. Chim. Acta* **1993**, *76*, 259–352.

45. Kaufmann, M.; Gisler, M.; Leumann, C. J., *Angew. Chem. Int. Ed. Engl.* **2009**, *48*, 3810-3813.

46. Nishio, M.; Hirota, M.; Umezawa, Y., The CH/π interaction. Evidence, nature, and consequences, Wiley-VCH, New York, NY, **1998**.

47. Tereshko, V.; Teplova, M.; Brunzelle, J.; Watterson, D. M.; Egli, M., *Nat. Struct. Biol.* **2001**, *8*, 899–907

48. Irimia, A.; Eoff, R. L.; Guengerich, F. P.; Egli, M., *J. Biol. Chem.* **2009**, *284*, 22467-22480.

49. Gehring, K.; Leroy, J. L.; Guéron, M., *Nature* **1993**, *363*, 561–565.

50. Chen, L.; Cai, L.; Zhang, X. H.; Rich, A., *Biochem.* **1994**, *33*, 13540–13546.

51. Berger, I.; Egli, M.; Rich, A., *Proc. Natl. Acad. Sci. U.S.A.* **1996**, *93*, 12116-12121.

52. Egli, M., In: Nucleic acids in chemistry and biology (Blackburn, G. M.; Gait, M. J.; Grasby, J. A.; Loakes, D.; Williams, D. M., eds.) Royal Society of Chemistry, Cambridge, UK, chapter 2, pp 13–75, **2006**.

53. Dougherty, D. A., *Science* **1996**, *271*, 163–168.

54. Ma, J. C.; Dougherty, D. A., *Chem. Rev.* **1997**, *97*, 1303–1324.

55. Lamoureux, J. S.; Maynes, J. T.; Glover, J. N. M., *J. Mol. Biol.* **2004**, *335*, 399–408.

56. Gallivan, J. P.; Dougherty, D. A., *Org. Lett.* **1999**, *1*, 103–105.

57. Scheiner, S.; Kar, T.; Pattanayek, J., *J. Am. Chem. Soc.* **2002**, *124*, 13257–13264.

58. Egli, M.; Gessner, R. V., *Proc. Natl. Acad. Sci. U.S.A.* **1995**, *92*, 180–184.

59. Reyes, A.; Fomina, L.; Rumsh, L.; Fomine, S., *Int. J. Quant. Chem.* **2005**, *104*, 335–341.

60. Jain, A.; Purohit, C. S.; Verma, S.; Sankaramakrishnan, R., *Chem. Phys. Lett. B* **2007**, *111*, 8680–8683.

61. Gessner, R. V.; Quigley, G. J.; Egli, M., *J. Mol. Biol.* **1994**, *236*, 1154–1168.

62. Wang, A. H. J.; Hakoshima, T.; van der Marel, G. A.; van Boom, J. H.; Rich, A., *Cell* **1984**, *37*, 321–331.

63. Egli, M.; Sarkhel, S., *Acc. Chem. Res.* **2007**, *40*, 197–205.

64. Bancroft, D.; Williams, L. D.; Rich, A.; Egli, M., *Biochem.* **1994**, *33*, 1073–1086.

65. Egli, M.; Minasov, G.; Su, L.; Rich, A., *Proc. Natl. Acad. Sci. U.S.A.* **2002**, *99*, 4302–4307.

66. Sarkhel, S.; Rich, A.; Egli, M., *J. Am. Chem. Soc.* **2003**, *125*, 8998–8999.

67. Ran, J.; Hobza, P., *J. Chem. Theory Comp.* **2009**, *5*, 1180–1185.

68. Yang, X.; Wu, D.; Ranford, J. D.; Vittal, J. J., *Crystal Growth and Design* **2005**, *5*, 41–43.

69. Mooibroek, T. J.; Gamez, P.; Reedijk, J., *Cryst. Eng. Comm.* **2008**, *10*, 1501–1515.

70. Jucker, F. M.; Pardi, A., *RNA* **1995**, *1*, 219–222.

71. de Hoog, P.; Gamez, P.; Mutikainen, I.; Turpeinen, U.; Reedijk, J., *Angew. Chem. Int. Ed. Engl.* **2004**, *43*, 5815–5817.

72. Demeshko, S.; Dechert, S.; Meyer, F., *J. Am. Chem. Soc.* **2004**, *126*, 4508–4509.

73. Rosokha, Y. S.; Lindeman, S. V.; Rosokha, S. V.; Kochi, J. K., *Angew. Chem. Int. Ed. Engl.* **2004**, *43*, 4650–4652.

74. Frontera, A.; Saczewski, F.; Gdaniec, M.; Dziemidowicz-Borys, E.; Kurland, A.; Deyà, P. M.; Quiñonero, D.; Garau, C., *Chem. Eur. J.* **2005**, *11*, 6560–6567

75. Schottel, B. L.; Chifotides, H. T.; Shatruk, M.; Chouai, A.; Pérez, L. M.; Bacsa, J.; Dunbar, K. R., *J. Am. Chem. Soc.* **2006**, *128*, 5895–5912.

76. Hobza, P.; Sponer, J., *Chem. Rev.* **1999**, *99*, 3247–3276.

77. Choi, M. Y.; Dong, F.; Miller, R. E., *Philos. Transact. A Math. Phys. Eng. Sci.* **2005**, *363*, 393–412.

78. Mukherjee, S.; Majumder, S.; Bhattacharyya, D., *J. Phys. Chem. B* **2005**, *109*, 10484–10492.

79. Choi, M. Y.; Miller, R. E., *J. Am. Chem. Soc.* **2006**, *128*, 7320–7328.

80. Choi, M. Y.; Dong, F.; Han, S. W.; Miller, R. E., *J. Phys. Chem. A* **2008**, *112*, 7185–7190.

81. Coll, M.; Frederick, C. A.; Wang, A. H. J.; Rich, A., *Proc. Natl. Acad. Sci. U.S.A.* **1987**, *84*, 8385–8389.

82. Sponer, J.; Hobza, P., *J. Am. Chem. Soc.* **1994**, *116*, 709–714.

83. Sponer, J.; Kypr, J., *Int. J. Biol. Macromol.* **1994**, *16*, 3–6.

196

84. Shatzky-Schwartz, M.; Arbuckle, N. D.; Eisenstein, M.; Rabinovich, D.; Bareket-Samish, A.; Haran, T. E.; Luisi, B. F.; Shakked, Z., *J. Mol. Biol.* **1997**, 267, 595–623.
85. Luisi, B.; Orozco, M.; Sponer, J.; Luque, F. J.; Shakked, Z., *J. Mol. Biol.* **1998**, *279*, 1123–1136.
86. Egli, M.; Tereshko, V.; Teplova, M.; Minasov, G.; Joachimiak, A.; Sanishvili, R.; Weeks, C. M.; Miller, R.; Maier, M. A.; An, H.; Cook, P. D.; Manoharan, M., *Biopolym. (Nucleic Acid Sci.)* **2000**, *48*, 234–252.
87. Smale, S. T.; Kadonaga, J. T., *Annu. Rev. Biochem.* **2003**, *72*, 449–479.
88. Guzikevich-Guerstein, G.; Shakked, Z., *Nat. Struct. Biol.* **1996**, *3*, 32–37.
89. Xiu, X.; Puskar, N. L.; Shanata, J. A. P.; Lester, H. A.; Dougherty, D. A., *Nature* **2009**, *458*, 534-537.